



A mathematical and numerical analysis of the Maxwell-Stefan diffusion equations

Laurent Boudin, Bérénice Grec, Francesco Salvarani

► To cite this version:

Laurent Boudin, Bérénice Grec, Francesco Salvarani. A mathematical and numerical analysis of the Maxwell-Stefan diffusion equations. *Discrete and Continuous Dynamical Systems - Series B*, 2012, 17 (5), pp.1427-1440. 10.3934/dcdsb.2012.17.1427 . hal-00490511

HAL Id: hal-00490511

<https://hal.science/hal-00490511>

Submitted on 8 Jun 2010

HAL is a multi-disciplinary open access archive for the deposit and dissemination of scientific research documents, whether they are published or not. The documents may come from teaching and research institutions in France or abroad, or from public or private research centers.

L'archive ouverte pluridisciplinaire **HAL**, est destinée au dépôt et à la diffusion de documents scientifiques de niveau recherche, publiés ou non, émanant des établissements d'enseignement et de recherche français ou étrangers, des laboratoires publics ou privés.

A MATHEMATICAL AND NUMERICAL ANALYSIS OF THE MAXWELL-STEFAN DIFFUSION EQUATIONS

LAURENT BOUDIN, BÉRÉNICE GREC, AND FRANCESCO SALVARANI

ABSTRACT. We consider the Maxwell-Stefan model of diffusion in a multicomponent gaseous mixture. After focusing on the main differences with the Fickian diffusion model, we study the equations governing a three-component gas mixture. We provide a qualitative and quantitative mathematical analysis of the model. The main properties of the standard explicit numerical scheme are also analyzed. We eventually include some numerical simulations pointing out the uphill diffusion phenomenon.

1. INTRODUCTION

Diffusion is a time-dependent process, originated by the motion of given entities that spread in space. The most classical description of the diffusion phenomenon goes back to Fick [10, 11]. He postulated that the flux goes from regions of high concentration to regions of low concentration, with a magnitude proportional to the concentration gradient. We refer to [4] for a general physical and mathematical overview of the Fickian diffusion.

The direct proportionality between flux and concentration gradient provides a reasonable approximation of the diffusion process in many common situations. Nevertheless, as experimentally observed, this postulate may be sometimes too simplistic. Indeed, there are some situations where the flux magnitude is not purely proportional to the concentration gradient or where the flux goes from regions of low concentration to regions of high concentration. The first behaviour has been recognized, for example, in porous media [5] and the second kind of behaviour has been observed, among other situations, in multicomponent gaseous mixtures (see [14] for a physical review on the model).

The diffusion phenomenon in a multicomponent gaseous mixture was first accurately described by Maxwell [16] and Stefan [18]. They suggested an explanation of the process based on the binary reciprocal interaction of the gas molecules. The result of their analysis is a system of coupled and nonlinear partial differential equations, and the diffusion happens in a much more complex way than the one foreseen by Fick's law.

Quite surprisingly, whereas the theory of the heat equation, based on Fick's law, is classical (see, for exemple, [9]), and there is a huge literature

on the mathematical properties of porous media-type equations [20], based on Darcy's law [5] and its generalizations, a complete mathematical study of the Maxwell-Stefan laws is still missing. Indeed, the main developments of the mathematical theory concerning the Maxwell-Stefan equations, up to now, are focused on the study of numerical algorithms based on the matricial description of the phenomenon [8, 7, 12, 13].

This article aims to contribute to fill the gap.

The paper is organized as follows. In the next section we briefly analyze the diffusion process in a gaseous mixture and then, in Section 3, we explain the physical derivation of the Maxwell-Stefan equations. A mathematical analysis of the system is then provided in Section 4 in the case of a ternary gaseous mixture. Finally, in Section 5, we propose a numerical scheme for the Maxwell-Stefan equations, for which we perform a numerical analysis and, in Section 6, we give some numerical results which emphasize the main features of the model, such as the uphill diffusion.

2. PHYSICS OF DIFFUSION IN GASEOUS MIXTURES

Let us consider a multicomponent gaseous mixture. The diffusion process of each species into the mixture is driven by a set of parameters, the binary diffusion coefficients (or binary diffusivities), which measure how a species diffuses in a volume filled out by another one thanks to a drag/friction force between the two species.

A celebrated experiment on a ternary gas mixture and the mutual diffusion of the species has been carried out by Duncan and Toor [6] in 1962. They studied an ideal gas mixture composed of hydrogen (H_2 , species 1), nitrogen (N_2 , species 2), and carbon dioxide (CO_2 , species 3) inside an isolated device. In this mixture, the binary diffusion coefficients are not equal. Indeed, we have

$$D_{12} = 83.3 \text{ mm}^2 \text{ s}^{-1}, \quad D_{13} = 68.0 \text{ mm}^2 \text{ s}^{-1}, \quad D_{23} = 16.8 \text{ mm}^2 \text{ s}^{-1}.$$

where D_{ij} denotes the binary diffusivity between species i and j , $i \neq j$.

Whereas the initial concentration of N_2 is constant in the whole device, the initial data for H_2 and CO_2 imply a strong concentration gradient.

Under the diffusion process, the high concentration gradients of carbon dioxide and hydrogen generate initially strong fluxes for these species. Due to the larger friction force between carbon dioxide and nitrogen (with respect to the pair hydrogen-nitrogen), carbon dioxide drags nitrogen, even though its concentration gradient is almost zero. This effect is called the *uphill diffusion*. It leads to a concentration gradient for nitrogen from the less concentrated region to the more concentrated one. Together with the decreasing fluxes of H_2 and N_2 , the mixture eventually reaches a point, called *diffusion barrier*, where this concentration gradient cancels out with the uphill diffusion effect. Beyond this point, the concentration gradient has a stronger effect than the friction forces and hence, the diffusion direction changes. The mixture asymptotically goes to the equilibrium, as it would

have happened for a mixture where Fick's law holds. The reader can refer to [2] for more modelling and computational details.

In order to understand why Fick's law fails in providing a reasonable description of the diffusion process in a gaseous mixture and, in particular, why the phenomenon of the uphill diffusion is not captured, it is necessary to take into account how the friction forces between different species influence the global behaviour of the mixture.

3. MAXWELL-STEFAN'S EQUATIONS

An ideal gaseous mixture, composed by $n \in \mathbb{N}$ species, is fully described by the mole fractions ξ_i of each species i , $1 \leq i \leq n$, and the total concentration c_{tot} of the mixture. Each mole fraction, which depends on time $t \geq 0$ and space location $x \in \mathbb{R}^d$, $d \in \mathbb{N}$, satisfies the continuity equation

$$\partial_t \xi_i + \nabla \cdot N_i = 0,$$

where $N_i = \xi_i u_i \in \mathbb{R}^d$ is the molar flux of species i , and u_i the molar velocity of that same species.

The relationships between the molar fluxes and the mole fractions depend on the diffusion model one chooses. In many cases, Fick's law provides a quite accurate physical description of the phenomenon but, as emphasized in Section 2, it does not allow to explain some behaviours which have been experimentally observed.

An explanation of such non-Fickian phenomena can be obtained by carefully studying the reciprocal action of the different species. The force acting on species i in a control volume is given by $-\nabla p_i$, where p_i is the partial pressure of that species in the mixture. In the case of an ideal gas mixture, the equation of state $p_i = RT c_{\text{tot}} \xi_i$ allows to deduce an explicit expression of the force per mole of species i , i.e. $-RT \nabla \xi_i / \xi_i$, where R denotes the ideal gas constant and T the absolute temperature.

At the equilibrium, this force is balanced by the drag/friction forces exerted by the other species in the mixture. Usually, the drag force is proportional to the relative velocity as well as to the mole fraction of the other components. The friction force between species i and j acting on species i then writes $RT \xi_j (u_i - u_j) / D_{ij}$. Here, u_i and u_j respectively denote the molar velocity of species i and j , and D_{ij} is the binary diffusion coefficient between the two species. For physical reasons, the binary diffusion coefficients satisfy the symmetry property $D_{ij} = D_{ji}$. The constant RT / D_{ij} can then be seen as a drag coefficient.

We can hence deduce the force balance for species i

$$-\frac{1}{\xi_i} \nabla \xi_i = \sum_{j \neq i} \frac{1}{D_{ij}} \xi_j (u_i - u_j).$$

If we multiply both sides of the previous equation by ξ_i , and use the relationship between N_i and u_i , we obtain

$$(1) \quad -\nabla \xi_i = \sum_{j \neq i} \frac{\xi_j N_i - \xi_i N_j}{D_{ij}}.$$

We note that there is a linear dependence between the Maxwell-Stefan laws (1) of all the species. Indeed, summing (1) over $1 \leq i \leq n$ implies that

$$(2) \quad \sum_{i=1}^n \nabla \xi_i = \left(\sum_{i=1}^n \sum_{j \neq i} \frac{\xi_j N_i}{D_{ij}} - \sum_{j=1}^n \sum_{i \neq j} \frac{\xi_i N_j}{D_{ij}} \right) = 0,$$

because of the symmetry property of the binary diffusion coefficients. Consequently, we have to add another equation to our system. When the convection is neglected, the behaviour of the mixture is purely diffusive. Hence the total sum of the fluxes is locally nil, i.e.

$$(3) \quad \sum_{i=1}^n N_i = 0,$$

which also ensures, with (2), the total mass conservation

$$(4) \quad \sum_{i=1}^n \xi_i = 1.$$

We observe that, when the binary diffusion coefficients are all equal, i.e. $D_{ij} = D \geq 0$ for all $1 \leq i, j \leq n$, thanks to (3)–(4), Maxwell-Stefan's law (1) reduces into Fick's law

$$N_i = -D \nabla \xi_i.$$

On the contrary, as shown by Duncan and Toor, when the binary diffusion coefficients are not of the same order of magnitude, Fick's law clearly becomes inaccurate to describe the physical behaviour of the system. It is hence necessary to treat the diffusion problem by using the full Maxwell-Stefan model.

It is worth noticing that, in this case, the PDEs satisfied by the mole fractions are coupled and, in general, nonlinear: indeed, because of (1), each flux is strongly related to the others and to all the mole fractions.

We refer to [14] for further considerations on the physical description of the Maxwell-Stefan diffusion. Note that the question explored in the article is not of pure academic nature, but is intended to be useful in the context of the lower respiratory airways, especially in the case of patients who suffer from a severe airway obstruction [3, 19, 2].

4. MATHEMATICAL PROPERTIES OF THE THREE-COMPONENT SYSTEM

In the previous sections, we have pointed out the peculiarity of the uphill diffusion. This feature is due to the coupling between the fluxes and the fact that at least a binary diffusion coefficient differs from the other ones.

Here we consider the simplest possible situation that exhibits the phenomenon of the uphill diffusion. We study the case of Duncan and Toor's experiment (hence, a ternary mixture) and suppose, moreover, that the two approximately equal binary diffusivity coefficients are, in fact, equal.

From a mathematical point of view, we are interested in the following problem:

$$(5) \quad \partial_t \xi_i + \nabla \cdot N_i = 0, \quad 1 \leq i \leq 3,$$

$$(6) \quad N_1 + N_2 + N_3 = 0,$$

$$(7) \quad \frac{\xi_2 N_1 - \xi_1 N_2}{D_{12}} + \frac{\xi_3 N_1 - \xi_1 N_3}{D_{13}} = -\nabla \xi_1,$$

$$(8) \quad \frac{\xi_1 N_2 - \xi_2 N_1}{D_{12}} + \frac{\xi_3 N_2 - \xi_2 N_3}{D_{23}} = -\nabla \xi_2,$$

posed in a bounded domain $\Omega \in \mathbb{R}^d$, $d \in \mathbb{N}$, with boundary $\partial\Omega$ of class C^1 . Note that (7) or (8) could have been replaced by the equation involving $-\nabla \xi_3$, because the three equations are linearly dependent, as stated in (2). The mole fractions satisfy the initial conditions

$$\xi_i(0, \cdot) = \xi_i^{\text{in}} \in L^\infty(\Omega), \quad 1 \leq i \leq 3,$$

where we have supposed that

$$\xi_i^{\text{in}} \geq 0, \quad 1 \leq i \leq 3, \quad \text{and} \quad \sum_{i=1}^3 \xi_i^{\text{in}} = 1.$$

As we already stated, that implies that

$$(9) \quad \sum_{i=1}^3 \xi_i = 1 \quad \text{on } \mathbb{R}_+ \times \Omega.$$

The boundary conditions are of no-flux type:

$$(10) \quad N_i = 0, \quad \text{on } \mathbb{R}_+ \times \partial\Omega, \quad 1 \leq i \leq 3.$$

Thanks to (6) and (9), (5)–(8) can be rewritten in the following reduced form, only using the two sets of unknowns (ξ_1, N_1) and (ξ_2, N_2) :

$$(11) \quad \partial_t \xi_i + \nabla \cdot N_i = 0, \quad 1 \leq i \leq 2,$$

$$(12) \quad \frac{1}{D_{13}} N_1 + \alpha N_1 \xi_2 - \alpha N_2 \xi_1 = -\nabla \xi_1,$$

$$(13) \quad \frac{1}{D_{23}} N_2 - \beta N_1 \xi_2 + \beta N_2 \xi_1 = -\nabla \xi_2,$$

where

$$\alpha = \left(\frac{1}{D_{12}} - \frac{1}{D_{13}} \right), \quad \beta = \left(\frac{1}{D_{12}} - \frac{1}{D_{23}} \right).$$

The unknown (ξ_3, N_3) and its properties can then be deduced from both other ones by using $\xi_3 = 1 - \xi_1 - \xi_2$ and $N_3 = -N_1 - N_2$. From now on, we focus on the reduced system involving species 1 and 2, i.e. (11)–(13). The associated initial conditions become

$$(14) \quad \xi_1(0, \cdot) = \xi_1^{\text{in}} \in L^\infty(\Omega), \quad \xi_2(0, \cdot) = \xi_2^{\text{in}} \in L^\infty(\Omega),$$

where

$$\xi_1^{\text{in}}, \xi_2^{\text{in}} \geq 0 \quad \text{and} \quad \xi_1^{\text{in}} + \xi_2^{\text{in}} \leq 1,$$

and the boundary conditions

$$(15) \quad N_1 = N_2 = 0, \quad \text{on } \mathbb{R}_+ \times \partial\Omega.$$

Let us also suppose that $D_{12} = D_{13}$, i.e. $\alpha = 0$. We do not make any assumption on β . In that situation, the terms involving α in (12) disappear, and N_1 and N_2 can be expressed by using ξ_1 and ξ_2 only, i.e.

$$(16) \quad N_1 = -D_{12} \nabla \xi_1,$$

$$(17) \quad N_2 = - \left(\frac{1}{D_{23}} + \beta \xi_1 \right)^{-1} (\nabla \xi_2 + \beta D_{12} \xi_2 \nabla \xi_1).$$

Note that, under that form, if $\beta = 0$, we clearly recover the Fickian expression of N_2 in (17). Hence we can deduce the equations that govern the mole fractions ξ_1 and ξ_2 without explicitly using the fluxes, i.e.

$$(18) \quad \partial_t \xi_1 = D_{12} \Delta \xi_1,$$

$$(19) \quad \partial_t \xi_2 = \nabla \cdot \left[\left(\frac{1}{D_{23}} + \beta \xi_1 \right)^{-1} (\nabla \xi_2 + \beta D_{12} \xi_2 \nabla \xi_1) \right].$$

The following result holds:

Proposition 4.1. *Let $\xi_1^{\text{in}}, \xi_2^{\text{in}}$ two non-negative functions in $L^\infty(\Omega)$ such that $\xi_1^{\text{in}} + \xi_2^{\text{in}} \leq 1$. The initial-boundary value problem (11)–(15), where $D_{12} = D_{13}$, admits unique smooth solutions (ξ_1, N_1) and (ξ_2, N_2) for all time. Moreover, ξ_1 and ξ_2 remain positive, and the mass of each species is conserved with respect to time, i.e.*

$$\|\xi_1(t, \cdot)\|_{L^1(\Omega)} = \|\xi_1^{\text{in}}\|_{L^1(\Omega)}, \quad \|\xi_2(t, \cdot)\|_{L^1(\Omega)} = \|\xi_2^{\text{in}}\|_{L^1(\Omega)}, \quad \forall t \in \mathbb{R}_+.$$

Proof. Existence, uniqueness, nonnegativity and regularity of the mole fraction ξ_1 are standard because it satisfies (18).

The same properties for the mole fraction ξ_2 follow by applying to (19) the results proved in [15, Chapter 4].

Indeed, since ξ_1 is solution of a heat equation, it appears as a parameter in (19), which is then uncoupled from the other equation. In fact, (19) can be reduced to a linear PDE of parabolic type in divergence form. Moreover, the boundary condition on N_2 clearly implies, using (17), a Neumann condition

on ξ_2 . Since $0 \leq \xi_1 \leq 1$ by the maximum principle of the heat equation (18), the term $(1/D_{23} + \beta\xi_1)$ of (19) is uniformly upper and lower bounded by two positive constants. Hence, (19) is uniformly parabolic: existence, uniqueness, nonnegativity and regularity of the mole fraction ξ_2 , as well the maximum principle, are then proved.

The molar fluxes are obtained directly by means of (16)–(17). The mass conservation of each species is a direct consequence of the integration with respect to x of the continuity equations (11), together with the initial and boundary conditions (14) and (15). \square

We now consider the problem of decay to equilibrium. We first obtain a preliminary result, which can be proven by direct inspection.

Lemma 4.2. *Let Ξ_1, Ξ_2 two positive constants such that $\Xi_1 + \Xi_2 \leq 1$. Then $(\Xi_1, 0)$ and $(\Xi_2, 0)$ are steady solutions to (11)–(13) with boundary conditions (15).*

We can then prove the following result:

Theorem 4.3. *Let $\xi_1^{\text{in}}, \xi_2^{\text{in}}$ two positive functions in $L^\infty(\Omega)$ such that $\xi_1^{\text{in}} + \xi_2^{\text{in}} \leq 1$. Consider (ξ_1, N_1) and (ξ_2, N_2) , the unique solutions of the initial-boundary value problem (11)–(15), where $D_{12} = D_{13}$.*

The mole fractions (ξ_i) asymptotically converge to

$$\bar{\xi}_i := \|\xi_i^{\text{in}}\|_{L^1(\Omega)} / \text{meas}(\Omega)$$

when t goes to $+\infty$. Moreover, let $K \geq 0$ a suitable constant depending on the binary diffusion coefficients, and set

$$H(t) = \frac{K}{2} \int_{\Omega} (\xi_1 - \bar{\xi}_1)^2 dx + \frac{1}{2} \int_{\Omega} (\xi_2 - \bar{\xi}_2)^2 dx.$$

Then the following estimate on the decay rate holds:

$$H(t) \leq H(0) \exp(-2\theta \min(D_{12}, D_{23}) C_{d,\Omega} t),$$

for any $\theta \in]0, 1[$, where $C_{d,\Omega}$ is the best constant of the Poincaré inequality on the domain $\Omega \in \mathbb{R}^d$.

Proof. Since ξ_1 satisfies (18), we immediately have

$$(20) \quad \frac{K}{2} \frac{d}{dt} \int_{\Omega} (\xi_1 - \bar{\xi}_1)^2 dx \leq -KD_{12} \int_{\Omega} |\nabla \xi_1|^2 dx.$$

We can write the same kind of inequality for ξ_2 , i.e.

$$(21) \quad \frac{1}{2} \frac{d}{dt} \int_{\Omega} (\xi_2 - \bar{\xi}_2)^2 dx \leq - \int_{\Omega} \gamma |\nabla \xi_2|^2 dx - \beta D_{12} \int_{\Omega} \gamma \xi_2 \nabla \xi_1 \cdot \nabla \xi_2 dx,$$

where

$$\gamma = \left(\frac{1}{D_{23}} + \beta \xi_1 \right)^{-1}.$$

Let $m = \min(D_{12}, D_{23})$ and $M = \max(D_{12}, D_{23})$. It is clear that $\gamma \in [m, M]$ on $\mathbb{R}_+ \times \Omega$. Using in (21) the standard inequality $ab \leq \varepsilon a^2 + b^2/4\varepsilon$, for any $\varepsilon > 0$, we get

$$(22) \quad \frac{1}{2} \frac{d}{dt} \int_{\Omega} (\xi_2 - \bar{\xi}_2)^2 dx \leq \varepsilon |\beta| D_{12} M \int_{\Omega} |\nabla \xi_1|^2 dx - \left[m - \frac{|\beta| D_{12} M}{4\varepsilon} \right] \int_{\Omega} |\nabla \xi_2|^2 dx.$$

By summing Equations (20) and (22), we obtain

$$H'(t) \leq -D_{12} (K - \varepsilon |\beta| M) \int_{\Omega} |\nabla \xi_1|^2 dx - \left(m - \frac{|\beta| D_{12} M}{4\varepsilon} \right) \int_{\Omega} |\nabla \xi_2|^2 dx.$$

Let $0 < \theta < 1$ and set

$$\varepsilon = \frac{|\beta| D_{12} M}{4(1 - \theta)m} > 0.$$

This choice obviously ensures that

$$m - \frac{|\beta| D_{12} M}{4\varepsilon} = \theta m > 0.$$

Then we choose

$$K = \frac{(\beta D_{12} M)^2}{4(1 - \theta)(D_{12} - \theta m)m} > 0,$$

so that

$$D_{12}(K - \varepsilon |\beta| M) = K\theta m > 0.$$

Consequently, we have

$$H'(t) \leq -\theta m \left(K \int_{\Omega} |\nabla \xi_1|^2 dx + \int_{\Omega} |\nabla \xi_2|^2 dx \right).$$

Thanks to Poincaré's inequality, we eventually get

$$H'(t) \leq -2\theta m C_{d,\Omega} H(t),$$

where $C_{d,\Omega}$ is the best constant (which only depends on the domain Ω and the dimension of the Euclidean space \mathbb{R}^d) of Poincaré's inequality. In particular, as shown by Payne and Weinberger [17] and by Bebendorf [1], $C_{d,\Omega} = \text{diam}(\Omega)/\pi$ for bounded, convex domains.

The required estimate is hence proved. \square

5. A NUMERICAL METHOD FOR THE 1-D MAXWELL-STEFAN EQUATIONS

In this section, we propose a finite-differences numerical scheme for the initial-boundary value problem (11)–(15).

Since we are mainly interested in exploring the phenomenon of uphill diffusion, we have chosen to work in a one-dimensional spatial setting.

In this case, indeed, all phenomena of mass displacement take place on the same straight line, and therefore the characterization of the uphill diffusion can be easily obtained by considering, locally in space and time, the sign of the product between the concentration gradient and the flux of each species.

Moreover, since non colinear phenomena do not occur, the one-dimensional case allows a better readability of the figures.

Hence, from now on, we will suppose that $\Omega = (0, 1)$.

In this section, if necessary, we exchange the species labels so that we can safely assume that $D_{23} \geq D_{13} \geq D_{12}$, i.e. $\alpha, \beta \geq 0$.

We consider a regular subdivision $(x_j)_{0 \leq j \leq J}$ of Ω , with $J \geq 1$. We set $\Delta x = 1/J > 0$, so that we have $x_j = j\Delta x$. The mole fractions ξ_i are computed at the centers $x_{j+1/2} := (j + 1/2)\Delta x$ of each interval $[x_j, x_{j+1}]$, $0 \leq j \leq J - 1$, whereas the corresponding molar fluxes N_i are computed at the nodes of the subdivision x_j , $0 \leq j \leq J$. Let us consider $\Delta t > 0$ without any further assumption for the moment. For each species $i \in \{1, 2\}$, we consider the approximations

$$\begin{aligned}\xi_i^{(k,j)} &\simeq \xi_i(k\Delta t, x_{j+1/2}), & k \in \mathbb{N}, \quad 0 \leq j \leq J - 1, \\ N_i^{(k,j)} &\simeq N_i(k\Delta t, x_j), & k \in \mathbb{N}, \quad 0 \leq j \leq J,\end{aligned}$$

and set

$$\xi_i^{(k,j-1/2)} = \frac{1}{2} \left(\xi_i^{(k,j)} + \xi_i^{(k,j-1)} \right), \quad k \in \mathbb{N}, \quad 1 \leq j \leq J - 1.$$

The initial-boundary value problem (11)–(15) can then be discretized as follows.

Discretization of (14)–(15), for $i \in \{1, 2\}$. We first take into account the initial and boundary conditions:

$$(23) \quad \xi_i^{(0,j)} = \xi_i^{\text{in}}(x_{j+1/2}), \quad 0 \leq j \leq J - 1$$

$$(24) \quad N_i^{(k,0)} = 0, \quad k \in \mathbb{N},$$

$$(25) \quad N_i^{(k,J)} = 0, \quad k \in \mathbb{N}.$$

Discretization of (12)–(13), for $i \in \{1, 2\}$. There is no time derivative in those equations, so we get a plain linear system of unknowns $N_1^{(k,j)} \Delta x$ and $N_2^{(k,j)} \Delta x$:

$$(26) \quad \left[\frac{1}{D_{13}} + \alpha \xi_2^{(k,j-1/2)} \right] N_1^{(k,j)} - \alpha \xi_1^{(k,j-1/2)} N_2^{(k,j)} = \frac{\xi_1^{(k,j-1)} - \xi_1^{(k,j)}}{\Delta x},$$

$$(27) \quad -\beta \xi_2^{(k,j-1/2)} N_1^{(k,j)} + \left[\frac{1}{D_{23}} + \beta \xi_1^{(k,j-1/2)} \right] N_2^{(k,j)} = \frac{\xi_2^{(k,j-1)} - \xi_2^{(k,j)}}{\Delta x},$$

for any $k \in \mathbb{N}$ and j , $1 \leq j \leq J - 1$. It can be solved with a standard Gauss elimination, and has unique solutions because the terms inside the brackets are both nonnegative.

Discretization of (11), for $i \in \{1, 2\}$. Eventually, we obtain the updated mole fractions by

$$(28) \quad \xi_i^{(k+1,j)} = \xi_i^{(k,j)} - \frac{\Delta t}{\Delta x^2} \left[N_i^{(k,j+1)} \Delta x - N_i^{(k,j)} \Delta x \right],$$

for any $k \in \mathbb{N}$ and j , $0 \leq j \leq J-1$.

5.1. Properties of the numerical scheme. The scheme (26)–(28) allowing to compute the mole fractions conserves the total masses $\|\xi_i(t)\|_{L_x^1}$, $i \in \{1, 2\}$. Indeed, using (24)–(25), we can check, for any $k \in \mathbb{N}$, that

$$\sum_{j=0}^{J-1} \xi_i^{(k+1,j)} = \sum_{j=0}^{J-1} \xi_i^{(k,j)} + \frac{\Delta t}{\Delta x^2} \sum_{j=0}^{J-1} \Delta x \left[N_i^{(k,j)} - N_i^{(k,j+1)} \right] = \sum_{j=0}^J \xi_i^{(k,j)}.$$

In the following, we investigate the consistency and stability of the scheme, and, we assume, as in Theorem 4.3, that $\alpha = 0$.

Proposition 5.1. *The numerical scheme defined by (23)–(28), where we choose $D_{12} = D_{13}$, is of first order in time and second order in space. Moreover, it is L^∞ -stable if*

$$(29) \quad D_{23} \frac{\Delta t}{\Delta x^2} \leq \frac{1}{2}.$$

Proof. Since ξ_1 satisfies a heat equation, the standard consistency orders are obtained and the corresponding stability condition is obviously satisfied because of (29), since $D_{12} \leq D_{13}$.

Let us denote

$$\sigma = \frac{\Delta t}{\Delta x^2}$$

and set, for $u, v \in [0, 1]$,

$$A(u, v) = \sigma D_{23} \frac{2 + \beta D_{12}(u - v)}{2 + \beta D_{23}(u + v)}.$$

One can check that

$$\begin{aligned} \frac{\partial A}{\partial u} &= -2\beta D_{23} \sigma \frac{(D_{23} - D_{12})(1 - v)}{[2 + \beta D_{23}(u + v)]^2} \leq 0, \\ \frac{\partial A}{\partial v} &= -2\beta D_{23} \sigma \frac{(D_{23} + D_{12}) + (D_{23} - D_{12})u}{[2 + \beta D_{23}(u + v)]^2} \leq 0. \end{aligned}$$

It is then easy to prove that

$$\sigma D_{12} \leq A(u, v) \leq \sigma D_{23}, \quad \forall u, v \in [0, 1].$$

Let us now set $X = \xi_1^{(k,j-1)}$, $Y = \xi_1^{(k,j)}$ and $Z = \xi_1^{(k,j+1)}$, which, as we already know, all lie in $[0, 1]$. We note that (28), for $i = 2$, can be rewritten using the function A :

$$\xi_2^{(k+1,j)} = (1 - A(Y, Z) - A(Y, X)) \xi_2^{(k,j)} + A(Z, Y) \xi_2^{(k,j+1)} + A(X, Y) \xi_2^{(k,j-1)}.$$

The fact that $\xi_2^{(k+1,j)}$ is still positive is then obvious if (29) holds.

Then we prove that $\xi_1^{(k,j)} + \xi_2^{(k,j)} \leq 1$ for any j , by induction on $k \in \mathbb{N}$. The case $k = 0$ is of course satisfied because $\xi_1^{\text{in}} + \xi_2^{\text{in}} \leq 1$ must hold. Now we assume that $\xi_1^{(k,j)} + \xi_2^{(k,j)} \leq 1$ for any j , and we prove the same property at iteration $k + 1$. We can easily write

$$\xi_1^{(k+1,j)} + \xi_2^{(k+1,j)} \leq F(X, Y, Z),$$

where F denotes

$$\begin{aligned} F(X, Y, Z) = (1 - 2\sigma D_{12})Y + \sigma D_{12}(X + Z) + (1 - A(Y, Z) - A(Y, X))(1 - Y) \\ + A(Z, Y)(1 - Z) + A(X, Y)(1 - X). \end{aligned}$$

After tedious but not difficult computations, it is possible to prove that $F(X, Y, Z) = 1$, which allows to obtain the required inequality. \square

Remark 5.2. When $\alpha \neq 0$, we numerically check that the scheme seems to remain stable if (29) holds, assuming that $D_{23} = \max D_{ij}$. In the following section, we obviously impose the stability condition on $\Delta t / \Delta x^2$.

6. NUMERICAL TESTS

We now use the numerical code proposed in Section 5 to explore the main features of the Maxwell-Stefan diffusion equations. The computations were performed using a numerical code written in C.

6.1. Asymptotic behaviour. In this subsection, we use $J = 100$. We proved in Theorem 4.3 that the mole fractions converge with an exponential rate towards the equilibrium, in the case when $\alpha = 0$. In fact, that exponential behaviour has been numerically recovered also for other values of α .

Let us consider the following initial data:

$$(30) \quad \xi_1^{\text{in}}(x) = \begin{cases} 0.8 & \text{if } 0 \leq x < 0.5 \\ 0 & \text{if } 0.5 \leq x \leq 1 \end{cases} \quad \text{and} \quad \xi_2^{\text{in}}(x) = 0.2, \quad \text{for all } x \in \Omega.$$

We first study the situation of the Duncan and Toor experiment, henceforth indicated as (DT), and choose the same values of the binary diffusion coefficients: $D_{12} = 0.833$, $D_{13} = 0.680$ and $D_{23} = 0.168$ (see Section 2). In Figure 1, we plot the quantity H defined in Theorem 4.3, for $K = 1$, with respect to time, and we clearly obtain an exponential convergence rate towards the equilibrium.

However, this behaviour may not hold anymore if we check the time evolution of an isolated species of the mixture. For example, if we consider the time evolution of the quantity $\|\xi_2 - \bar{\xi}_2\|_{L^2(\Omega)}^2$, we can see on Figure 2 that the exponential convergence only takes place after a transient period: the reciprocal interaction with the other species of the mixture induces a temporary growth of the aforementioned quantity, and only after some time the density tend to the expected asymptotic profile, which was exactly coincident with the initial condition.

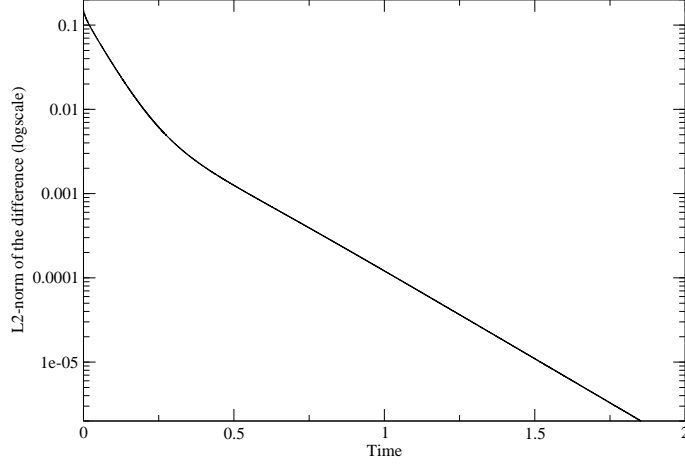


FIGURE 1. Asymptotic behaviour for the (DT)-situation: time evolution of $H(t)$ for $K = 1$

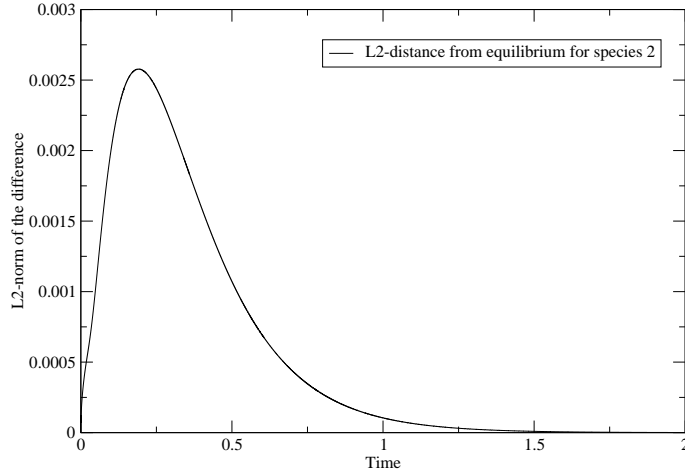


FIGURE 2. $\|\xi_2 - \bar{\xi}_2\|_{L^2(\Omega)}^2$ w.r.t. time.

6.2. Uphill diffusion. We are here interested in the phenomenon of uphill diffusion. We investigate a situation close to the Duncan and Toor experiment, where we choose $D_{12} = D_{13} = 0.833$ ($\alpha = 0$) and $D_{23} = 0.168$. This case will be indicated as the *semi-degenerate Duncan and Toor experiment* (SDDT). The computations are performed with $J = 140$. We consider two sets of initial data. The first one is given by (30), and the second one is

continuous:

(31)

$$\xi_1^{\text{in}}(x) = \begin{cases} 0.8 & \text{if } 0 \leq x < 0.25 \\ 1.6(0.75 - x) & \text{if } 0.25 \leq x < 0.75, \\ 0 & \text{if } 0.75 \leq x \leq 1 \end{cases}, \quad \xi_2^{\text{in}}(x) = 0.2 \text{ for all } x \in \Omega.$$

The initial datum in (31) for ξ_1 appears as a smoothed version of the one in (30).

On Figure 3, we plot the space-time region where the concentration gradient of the species experiencing the uphill diffusion (here, species 2) and the corresponding flux share the same sign.

The asymmetrical shapes of the uphill diffusion regions can be explained by the asymmetry of the initial data. We observe that in both figures, the uphill diffusion zone for ξ_2 begins at the variations of the initial values for ξ_1 and ξ_3 (i.e. the jumps of ξ_1 and ξ_3 or their derivatives). Indeed, it corresponds to the zone of the strongest flux of ξ_1 and ξ_3 , which drags species 2 and causes its uphill diffusion. Thus, for small times, the space-time regions of uphill diffusion are quite different, whereas, when we get closer to time 0.2, the shapes of the regions look quite similar. Eventually, the uphill diffusion phenomenon is localized in space and tends to be shifted towards the areas which were initially at the equilibrium. Beyond $t = 0.27$, the uphill diffusion phenomenon disappears everywhere.

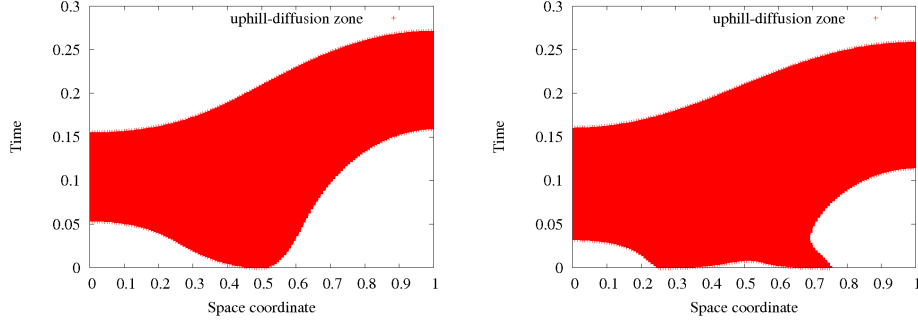


FIGURE 3. Space-time region where $N_2 \partial_x \xi_2 \geq 0$ (a) for (30), and (b) for (31)

We note that, for the initial conditions (31), there are some regions where uphill diffusion happens in two non-connected time intervals (see in Figure 3b), which induces, by comparison with Figure 3a, a significant difference in the topological form of the uphill diffusion areas. In fact, this proves that at a given point, uphill diffusion can happen more than once. In order to understand better the physical factors leading to this fact, we plot on Figure 4 both the flux of ξ_2 and the opposite of its concentration gradient at $x = 0.72$ with respect to time.

We recover the two separated time intervals of uphill diffusion. Actually, we observe that there is only one sign change for the flux, and the two intervals of uphill diffusion are due to two sign changes for the concentration gradient. These sign changes are caused by the complex movement of the other species ξ_1 and ξ_3 depending on the initial data.

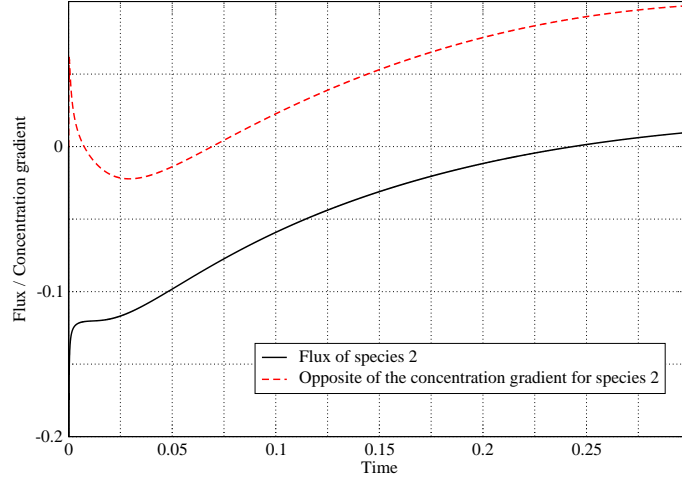


FIGURE 4. Uphill diffusion for (31): N_2 and $-\partial_x \xi_2$ w.r.t. t at $x = 0.72$

Acknowledgements. This work was partially funded by the French ANR-08-JCJC-013-01 project headed by C. Grandmont.

REFERENCES

- [1] M. Bebendorf. A note on the Poincaré inequality for convex domains. *Z. Anal. Anwendungen*, 22(4):751–756, 2003.
- [2] L. Boudin, D. Götz, and B. Grec. Diffusive models for the air in the acinus. *ESAIM Proc.*, 2010. To be published.
- [3] H.K. Chang. Multicomponent diffusion in the lung. *Fed. Proc.*, 39(10):2759–2764, 1980.
- [4] J. Crank. *The mathematics of diffusion*. Clarendon Press, Oxford, second edition, 1975.
- [5] H. Darcy. *Les fontaines publiques de la ville de Dijon*. V. Dalmont, Paris, 1856.
- [6] J. B. Duncan and H. L. Toor. An experimental study of three component gas diffusion. *AIChE Journal*, 8(1):38–41, 1962.
- [7] A. Ern and V. Giovangigli. *Multicomponent transport algorithms*, volume 24 of *Lecture Notes in Physics. New Series M: Monographs*. Springer-Verlag, Berlin, 1994.
- [8] A. Ern and V. Giovangigli. Projected iterative algorithms with application to multicomponent transport. *Linear Algebra Appl.*, 250:289–315, 1997.
- [9] L. C. Evans. *Partial differential equations*, volume 19 of *Graduate Studies in Mathematics*. American Mathematical Society, Providence, RI, second edition, 2010.
- [10] A. Fick. On liquid diffusion. *Phil. Mag.*, 10(63):30–39, 1855.
- [11] A. Fick. Ueber Diffusion. *Poggendorff's Annal Physik*, 94:59–86, 1855.

- [12] V. Giovangigli. Convergent iterative methods for multicomponent diffusion. *Impact Comput. Sci. Engrg.*, 3(3):244–276, 1991.
- [13] V. Giovangigli. *Multicomponent flow modeling*. Modeling and Simulation in Science, Engineering and Technology. Birkhäuser Boston Inc., Boston, MA, 1999.
- [14] R. Krishna and J. A. Wesselingh. The Maxwell-Stefan approach to mass transfer. *Chem. Eng. Sci.*, 52(6):861–911, 1997.
- [15] O. A. Ladyženskaja, V. A. Solonnikov, and N. N. Ural'ceva. *Linear and quasilinear equations of parabolic type*. American Mathematical Society, Providence, R.I., 1967.
- [16] J. C. Maxwell. On the dynamical theory of gases. *Phil. Trans. R. Soc.*, 157:49–88, 1866.
- [17] L. E. Payne and H. F. Weinberger. An optimal Poincaré inequality for convex domains. *Arch. Rational Mech. Anal.*, 5:286–292 (1960), 1960.
- [18] J. Stefan. Ueber das Gleichgewicht und die Bewegung insbesondere die Diffusion von Gasgemengen. *Akad. Wiss. Wien*, 63:63–124, 1871.
- [19] M. Thiriet, D. Douguet, J.-C. Bonnet, C. Canonne, and C. Hatzfeld. The effect on gas mixing of a He-O₂ mixture in chronic obstructive lung diseases. *Bull. Eur. Physiopathol. Respir.*, 15(5):1053–1068, 1979. In French.
- [20] J. L. Vázquez. *The porous medium equation*. Oxford Mathematical Monographs. The Clarendon Press Oxford University Press, Oxford, 2007. Mathematical theory.

L.B.: UPMC UNIV PARIS 06, UMR 7598 LJLL, PARIS, F-75005, FRANCE & INRIA PARIS-ROCQUENCOURT, REO PROJECT TEAM, BP 105, F-78153 LE CHESNAY CEDEX, FRANCE

E-mail address: laurent.boudin@upmc.fr

B.G.: MAP5, CNRS UMR 8145, UNIVERSITÉ PARIS DESCARTES, F-75006 PARIS, FRANCE

E-mail address: berenice.grec@parisdescartes.fr

F.S.: INRIA PARIS-ROCQUENCOURT, REO PROJECT TEAM, BP 105, F-78153 LE CHESNAY CEDEX, FRANCE & DIPARTIMENTO DI MATEMATICA, UNIVERSITÀ DEGLI STUDI DI PAVIA, VIA FERRATA 1 - I-27100 PAVIA, ITALY

E-mail address: francesco.salvarani@unipv.it